J|A|C|S
ARTICLES
Published on Web 08/21/2007

Characterization of a Genuine Iron(V)−Nitrido Species by Nuclear Resonant Vibrational Spectroscopy Coupled to Density Functional Calculations

Taras Petrenko,[†] Serena DeBeer George,*[,‡] Núria Aliaga-Alcalde,[§] Eckhard Bill,[§] Bernd Mienert,[§] Yuming Xiao,[||] YiSong Guo,[||] Wolfgang Sturhahn,[⊥] Stephen P. Cramer,[||,#] Karl Wieghardt,[§] and Frank Neese*[,†]

Contribution from the Institut für Physikalische und Theoretische Chemie, Wegelerstr. 12, D-53115 Bonn, Germany, Stanford Synchrotron Radiation Laboratory, SLAC, Stanford University, Stanford, California 94309, Max-Planck Institut für Bioanorganische Chemie, Stiftstr. 34-36; D-45470 Mülheim an der Ruhr, Germany, Department of Applied Science, University of California Davis, Davis, California 95616, Advanced Photon Source, Argonne National Laboratory, Argonne, Illinois 60439, and Physical Biosciences Division, Lawrence Berkeley National Laboratory, Berkeley, California 94720

Received February 3, 2007; E-mail: debeer@stanford.edu; neese@thch.uni-bonn.de

Abstract: The characterization of high-valent iron species is of interest due to their relevance to biological reaction mechanisms. Recently, we have synthesized and characterized an [Fe(V)-nitrido-cyclam-acetato]$^+$ complex, which has been characterized by Mössbauer, magnetic susceptibility data, and XAS spectroscopies combined with DFT calculations (Aliaga-Alcade, N.; DeBeer George, S.; Bill, E.; Wieghardt, K.; Neese, F. *Angew. Chem., Int. Ed.* **2005**, *44*, 2908−2912). The results of this study indicated that the [Fe(V)-nitrido-cyclam-acetato]$^+$ complex is an unusual d^3 system with a nearly orbitally degenerate $S = {}^1/_2$ ground state. Although the calculations predicted fairly different Fe−N stretching frequencies for the $S = {}^1/_2$ and the competing $S = {}^3/_2$ ground states, a direct experimental determination of this important fingerprint quantity was missing. Here we apply synchrotron-based nuclear resonance vibrational scattering (NRVS) to characterize the Fe−N stretching frequency of an Fe(V)−nitrido complex and its Fe(III)−azide precursor. The NRVS data show a new isolated band at 864 cm^{-1} in the Fe(V)−nitrido complex that is absent in the precursor. The NRVS spectra are fit and simulated using a DFT approach, and the new feature is unambiguously assigned to a Fe(V)−N stretch. The calculated Fe−N stretching frequency is too high by ∼75 cm^{-1}. Anharmonic contributions to the Fe−N stretching frequency have been evaluated and have been found to be small (−5.5 cm^{-1}). The NRVS data provided a unique opportunity to obtain this vibrational information, which had eluded characterization by more traditional vibrational spectroscopies.

Introduction

High-valent iron intermediates have been invoked as the active oxidizing species in the catalytic cycles of numerous iron-containing enzymes.[1−3] These include, for example, the heme iron sites in cyctochrome P450, peroxidase, and catalase, and the non-heme sites in methane monoxygenase, ribonucleotide reductase, and taurine:α-ketoglutarate dioxygenase. The importance and the diversity of the reactions carried out by these enzymes have driven inorganic chemists to synthesize and spectroscopically characterize high-valent iron model complexes in an effort to obtain insight into the enzymatic mechanisms.

Recent work in our laboratory has focused on the synthesis of high-valent iron species by photolysis of lower valent Fe−azide precursors,[4−6] as shown in Scheme 1.

Using an Fe(III)−azide(cyclam-acetato) complex (**1**), an Fe(V) species can be generated by photolysis with 420 nm light, producing a formally Fe(V)−nitrido(cyclam-acetato) complex (**2**). This photolysis product has been investigated through detailed spectroscopic studies, which have included Mössbauer, magnetic susceptibility, and XAS.[7] The results of these experiments, combined with DFT calculations, were important in establishing that this species is a genuine Fe(V) complex with an unexpected $S = {}^1/_2$ ground state (^{2}**2**) (as opposed to the canonical $S = {}^3/_2$ (^{4}**2**), which would generally be assumed for an octahedral d^3 system). DFT calculations have demonstrated

[†] Institut für Physikalische und Theoretische Chemie.
[‡] Stanford University.
[§] Max-Planck Institut für Bioanorganische Chemie.
[||] University of California Davis.
[⊥] Argonne National Laboratory.
[#] Lawrence Berkeley National Laboratory.

(1) Slep, L. D.; Neese, F. *Angew. Chem., Int. Ed.* **2003**, *42*, 2942.
(2) Costas, M.; Mehn, M. P.; Jensen, M. P.; Que, L., Jr. *Chem. Rev.* **2004**, *104*, 939.
(3) Harris, D. L. *Curr. Op. Chem. Biol.* **2001**, *5*, 724.
(4) Meyer, K.; Bill, E.; Mienert, B.; Weyhermüller, T.; Wieghardt, K. *J. Am. Chem. Soc.* **1999**, *121*, 4859.
(5) Grapperhaus, C. A.; Mienert, B.; Bill, E.; Weyhermüller, T.; Wieghardt, K. *Inorg. Chem.* **2000**, *39*, 5306.
(6) Berry, J. F.; Bill, E.; Bothe, E.; DeBeer George, S.; Mienert, B.; Neese, F.; Wieghardt, K. *Science* **2006**, *312*, 1937.
(7) Aliaga-Alcalde, N.; DeBeer George, S.; Mienert, B.; Bill, E.; Wieghardt, K.; Neese, F. *Angew. Chem., Int. Ed.* **2005**, *44*, 2908.

Scheme 1

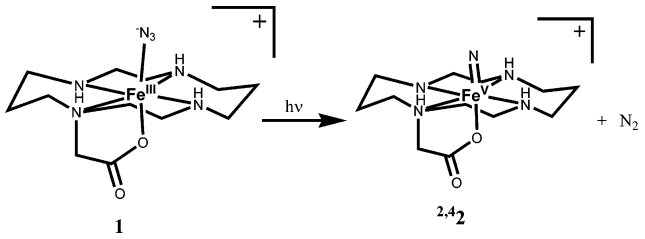

that these two ground states would differ significantly, with a 1.61 Å Fe−N(nitrido) bond and 937 cm^{-1} υ(Fe−N) for ^{2}**2**, and a 1.74 Å Fe−N(nitrido) bond and 671 cm^{-1} ν(Fe−N) for ^{4}**2**. EXAFS data have confirmed the 1.61 Å Fe−N bond length; however, vibrational data establishing the Fe−N(nitrido) stretching frequency was absent, despite attempts to obtain these data by conventional vibrational spectroscopy.[8]

Here, we apply a synchrotron-based vibrational method known as nuclear resonance vibrational scattering (NRVS)[9,10] to experimentally probe the Fe−N(nitrido)stretch in complex **2** and in the azide precursor **1**. NRVS utilizes a high resolution (∼1 meV) incident X-ray beam which is tuned to the ^{57}Fe nuclear transition energy. By scanning the incident beam relative to the Mössbauer resonance, side-bands are observed that correspond to the nuclear transition in combination with excitation or de-excitation of vibrational modes. This method has been successfully applied to heme proteins[11,12] and models,[13−16] iron-sulfur proteins,[17] and most recently to the FeMo-cofactor in nitrogenase.[18] The advantage of NRVS is that it selects only for those vibrations that involve a displacement of the resonant nucleus (^{57}Fe), and thus provides a very sensitive probe of Fe dynamics. This has led to the selective observation of Fe vibrations, which though allowed, have not been reported in resonance Raman studies.[10] In this study, we report the first NRVS characterization of a high-valent Fe species. These data also represent some of the highest frequency NRVS data that have been reported, which is significant due to the 1/energy dependence of the scattering probability.[45] These data provide the unique opportunity to experimentally measure the Fe−N stretching frequency of complex **2**, and thus allow the $S = {}^1/_2$ (^{2}**2**) and $S = {}^3/_2$ (^{4}**2**) ground states to be unambiguously distinguished. Using a DFT approach, the normal mode composition factors and vibrational frequencies have been determined, and the NRVS spectra have been fitted and simulated. The strong correlation between the experimental and calculated spectra allows for a clear interpretation of the NRVS data. These data provide important spectroscopic markers for high-valent Fe species and demonstrate the utility of this technique for the determination of Fe dynamics.

Materials and Methods

Synthesis. The tetrahydrochloride salt of the ligand 1,4,8,11-tetraazacyclotetradecane-1-acetic acid (cyclam-acetate) and the ferric azide starting complex [(cyclam-acetato)^{57}FeN_3]PF_6 were synthesized according to published methods.[4,5] The enrichment of ^{57}Fe (∼95%) in the material was confirmed by electrospray ionization mass spectrometry.

Sample Preparation and Photolysis. Two equivalent aliquots of ^{57}Fe-enriched solid powder (∼50 mg) were loaded in to two 3 × 7 × 1 mm^3 Lucite NRVS cells. The layers of fine powder material were stabilized with a drop of hexane prior to freezing in liquid nitrogen. The sample layer is ∼1 mm thick and the active window for NRVS fluorescence measurements is 2 × 5 mm^2, with an ∼0.16 mm thick Lucite window. In one cell, the precursor **1** was photolyzed at 77 K with a high-pressure mercury lamp (Osram, HBO 200W, in a Schoeffel mount), whereas the other cell was left untreated for reference. A collimation lens focused light on the illuminated cell, which was kept immersed in liquid nitrogen during the entire procedure. Edge filters were used to cutoff the illumination spectrum at 420 nm and about 1500 nm, respectively, to prevent sample damage from intense UV radiation and excessive heating. Illumination was for 20 h through the Lucite window, as well as 20 h through the 0.5 mm thick, opaque Lucite back wall. The purity of the samples and the photolytic conversion yield were monitored by conventional transmission ^{57}Fe Mössbauer spectroscopy before and after the NRVS measurement. The samples were shipped in a liquid nitrogen dewar to the synchrotron site.

Mössbauer Spectroscopy. Transmission Mössbauer data were recorded on a conventional spectrometer operating in alternating constant-acceleration mode. The minimum experimental line width was 0.24 mm s^{-1} (full width at half-height). A constant sample temperature was maintained with an Oxford Instruments Variox cryostat. The ^{57}Co/Rh source (≈ 0.6 GBq) was at room temperature. Reported isomer shifts (δ) are referenced versus iron metal at 300 K.

Nuclear Resonance Vibrational Spectroscopy (NRVS). NRVS spectra were recorded as described in reference,[9] using beam line 3-ID at the Advanced Photon Source (APS).[19] Beam line 3-ID provides ∼2.5 × 10^9 photons/sec in ∼1 meV bandwidth at 14.4125 keV in a 0.5 mm (vertical) × 0.5 mm (horizontal) spot. A water-cooled diamond double crystal monochromator with 1.1 eV bandpass is followed by a high-resolution monochromator consisting of two asymmetrically cut Si (4 0 0) and two asymmetrically cut Si (10 6 4) crystals, respectively. The design of the high-resolution monochromator and the artificial channel-cut arrangement were described earlier.[19,20] During the NRVS measurements, the samples were maintained at cryogenic temperatures using liquid He. Because the cryostat temperature sensor was not directly in contact with the samples, the exact temperatures for individual spectra are not precisely known. In principle, the ratio of Stokes to anti-Stokes intensities could establish the temperature well if anti-Stokes bands were detectable. This was not the case in the present study because the isolated low-frequency (<100 cm^{-1}) anti-Stokes bands were not well-resolved, and the high-frequency anti-Stokes bands (>100 cm^{-1}) had negligible intensities. However, the estimated temperature uncertainty of ∼10 K has not affected the results of the present analysis of the NRVS intensities in the 130−1000 cm^{-1} spectral range, because the

(8) Our attempts to observe the Fe−N stretching frequency [Garcia-Serres, R. Ph.D. thesis, University of Bochum, Department of Chemistry, 2002] suffered from the low-intensity of the Fe−N stretch. Preliminary calculations suggested that this might be due to the limited polarity of the Fe(V)−N bond as opposed to the significantly polar Mn(V)−N bond where the Mn−N stretch is readily observed [ref 40, 41].
(9) Sturhahn, W. *J. Phys. Condens. Matter* **2004**, *16*, S497.
(10) Scheidt, W. R.; Durbin, S. M.; Sage, J. T. *J. Inorg. Biochem.* **2005**, *99*, 60.
(11) Adams, K. L.; Tsoi, S.; Yan, J.; Durbin, S. M.; Ramdas, A. K.; Cramer, W. A.; Sturhahn, W.; Alp, E. E.; Schulz, C. *J. Phys. Chem. B.* **2006**, *110*, 530.
(12) Zeng, W.; Silvernail, N. J.; Wharton, D. C.; Georgiev, G. Y.; Leu, B. M.; Scheidt, W. R.; Zhao, J.; Sturhahn, W.; Alp, E. E.; Sage, J. T. *J. Am. Chem. Soc.* **2005**, *127*, 11200.
(13) Rai, B. K.; Durbin, S. M.; Prohofsky, E. W.; Sage, J. T.; Wyllie, G. R. A.; Scheidt, W. R.; Sturhahn, W.; Alp, E. E. *Biophys. J.* **2002**, *82*, 2951.
(14) Rai, B. K.; Durbin, S. M.; Prohofsky, E. W.; Sage, J. T.; Ellison, M. K.; Roth, A.; Scheidt, W. R.; Sturhahn, W.; Alp, E. E. *J. Am. Chem. Soc.* **2003**, *125*, 6927.
(15) Budarz, T. O.; Prohofsky, E. W.; Durbin, S. M.; Sjodin, T.; Sage, J. T.; Sturhahn, W.; Alp, E. E. *J. Phys. Chem. B.* **2003**, *107*, 11170.
(16) Starovoitova, V.; Budarz, T. O.; Wyllie, G. R. A.; Scheidt, W. R.; Sturhahn, W.; Alp, E. E.; Prohofsky, E. W.; Durbin, S. M. *J. Phys. Chem. B.* **2006**, *110*, 13277.
(17) Xiao, Y.; Wang, H.; George, S. J.; Smith, M. C.; Adams, M. W. W.; Jenney, F. E., Jr.; Sturhahn, W.; Alp, E. E.; Zhao, J.; Yoda, Y.; Dey, A.; Solomon, E. I.; Cramer, S. P. *J. Am. Chem. Soc.* **2005**, *127*, 14596.
(18) Xiao, Y.; Fisher, K.; Smith, M. C.; Newton, W. E.; Case, D. A.; George, S. J.; Wang, H.; Sturhahn, W.; Alp, E. E.; Zhao, J.; Yoda, Y.; Cramer, S. P. *J. Am. Chem. Soc.* **2006**, *128*, 7608.
(19) Toellner, T. S. *Hyperfine Interact.* **2000**, *125*, 3.
(20) Shu, D.; Toellner, T. S.; Alp, E. E. In *Synchrotron Radiation Instrumentation: 11th US National Conference Proceedings*; Pianetta, P., Ed.; AIP: Woodbury, NY, 2000; Vol. 521, p 219.

intensities are not very sensitive to temperature variations in the 0−50 K range. Thus, the largest intensity changes of ∼1% were found for the low-frequency modes at ∼150 cm^{-1}. Spectra were recorded between −25 and 125 meV in steps of 0.25 meV. Delayed nuclear fluorescence and Fe K fluorescence were recorded with a single avalanche photodiode.[21] Each scan took ∼70 min, and all scans were added and normalized to the intensity of the incident beam. The data represent 7- and 10-scan averages for the precursor **1** and the photolysis product **2**, respectively.

Electronic Structure Calculations. Electronic structure calculations were performed with the program package ORCA developed in our laboratory.[22] Structures of **1**, ^{2}**2**, and ^{4}**2** were optimized at the BP86 level of DFT.[23,24] with polarized triple-ζ basis sets.[25] Calculation of the harmonic force fields of all species at the same level proved all structures to be local minima on the potential energy surface and provided vibrational frequencies and normal mode compositions used to calculate parameters for NRVS spectra simulations. Total electronic energies were calculated with the TZVPP basis set[26] and the B3LYP functional.[27,28] Mössbauer parameters were calculated as described in previous publications.[29] Environmental effects were modeled with the conductor-like screening model (COSMO) as implemented in ORCA and using acetonitrile ($\epsilon = 36.6$) as solvent. The calculation of NRVS spectra and partial vibrational density of states has been implemented in a general way in the course of this work and are publicly available in the current release of the ORCA package. The implemented theory is described in the Supporting Information.

Results

Mössbauer. We recorded zero-field Mössbauer spectra from the highly ^{57}Fe-enriched (95%) powder sample of **1**(PF_6) as it was prepared and photolyzed in the NRVS cell in order to probe its purity and the yield of photolytic conversion, as well as to detect possible radiation damage during the NRVS measurements. For comparison, an identically prepared untreated sample was also measured. The untreated sample, **1**, showed a very intense, almost symmetric line doublet that could be reasonably well fit with a quadrupole doublet with Lorentzian line shape, an isomer shift $\delta = 0.27$ mm/s, and quadrupole splitting $\Delta E_Q = 2.30$ mm/s (Figure S1, top, see Supporting Information). These values correspond to the values previously found for the azide starting complex **1** in frozen acetonitrile solution[5] and render the ferric ion in low-spin state. In addition, a weak subspectrum was found with $\delta = 0.46$ mm/s and $\Delta E_Q = 0.74$ mm/s, which is assigned to a minor contribution from a ferric-μ-oxo dimer contaminant. From the Lorentzian fit, its relative intensity is ∼3.7%, but this may be an overestimate (by a factor ∼2) due to strong saturation effects in the highly enriched sample (as discussed below).

Photolysis of the first NRVS sample for ∼42 h attenuated the low-spin spectrum and yielded a new Mössbauer subspectrum with parameters $\delta = -0.03$ mm/s and $\Delta E_Q = 1.64$ mm/s, which is typical of the high-valent [(cyclam-acetato)^{57}Fe(V)═N]$^+$ target complex **2** (Figure S1, middle). Almost identical parameters have been observed previously for this iron(V)nitrido species generated in frozen acetonitrile solution ($\delta = -0.04$ mm/s and $\Delta E_Q = 1.67$ mm/s).[5] The photolyzed NRVS sample showed no changes other than formation of this species. In particular, absolutely no formation of ferrous iron could be detected. Thus, photoreduction did not occur under the present illumination conditions of the solid powder sample.

It is difficult to determine the exact conversion ratio of **1** to **2.** Due to the high enrichment factor, dramatic saturation effects obscure the relative line intensities. The basic fit with Lorentzian lines yielded apparent relative intensities of only 19% for the high-valent species **2** in the bulk NRVS sample. This is even an overestimate of the true abundance of **2**, since the dominant lines from the ferric starting complex **1** are more saturated than the weak subspectrum from the iron(V) target **2**. We derived a crude correction factor for this value from the effective thickness of the sample and the related relative fractional absorbances[30] for the strong and the weak subspectra. The effective thickness of the sample according to metric dimensions, amount of material, and the enrichment can be estimated to be approximately $t \approx 42$ for each line of the starting complex before illumination (adopting a Lamb-Mössbauer factor of the absorber (f_{abs}) of 0.8 and 30% heterogeneous broadening). This yields an expected relative fraction absorbance of $\epsilon = 0.91$ for the untreated ferric starting spectrum. A corresponding estimate for the minority Fe(V) species and comparison of the ϵ values with the measured data yielded roughly a rather low total of 10% true abundance for the iron(V) compound in the photolyzed sample.

However, it is likely that the amount of target material sensed by the NRVS experiments is much higher than 10% for two reasons. First, the detection setup of NRVS yields strong surface sensitivity (relative to conventional transmission Mössbauer), and second we know from visual inspection of other photolysis samples that the penetration depth of our illumination in solid powder samples is very short, clearly in the submillimeter range. This range probably matches quite well the sample layer that is effectively probed by NRVS, because detection of NRVS is primarily based on scattered Fe K_α-X-rays as they arise from the high internal conversion for the exited ^{57}Fe nucleus. Their penetration depth is short due to their low energy (6 keV). We estimate that the concentration of the iron(V) nitrido species in the effectively probed sample surface layer may be of the order 30−50% for the NRVS spectra. Such a high value is also consistent with the results of the direct theoretical calculations of the NRVS spectra.

After the NRVS measurement, zero-field Mössbauer spectra have been recorded again for the same samples, without detecting any measurable changes. Thus, in summary, the conventional Mössbauer spectra establish the purity of the ferric starting complex [(cyclam-acetato)^{57}FeN_3]PF_6 (**1**) and the exclusive, clean photolytic production of the [(cyclam-acetato)^{57}Fe(V)═N]$^+$ target complex (**2**) in sizable yield and the complete absence of photoreduction products.

NRVS. Figure 1 shows the NRVS signal for the Fe(III)−azide precursor and the converted photolysis product. Due to incomplete conversion of the photolyzed sample, both spectra exhibit rather similar features in the 100−600 cm^{-1} region, with noticeable changes around 300 cm^{-1} attributed to the presence of **2**. However, despite the incomplete conversion, there is a significant change observed at higher frequency upon photolysis, namely, the appearance of a well-isolated new band at 864 cm^{-1}.

(21) Baron, A. Q. R.; Kishimoto, S.; Morse, J.; Rigal, J.-M. *J. Synchrotron Radiat.* **2006**, *13*, 131−142.
(22) Neese, F. *ORCA-an ab inito DFT and Semiempirical Electronic Structure Package*, version 2.5.30; University of Bonn Germany, 2007.
(23) Becke, A. D. *Phys. Rev. A* **1988**, *38*, 3098.
(24) Perdew, J. P. *Phys. Rev. B* **1986**, *33*, 8822.
(25) Schäfer, A.; Huber, C.; Ahlrichs, R. *J. Chem. Phys.* **1994**, *100*, 5829.
(26) TURBOMOLE library: ftp://ftp.chemie.uni-karlsruhe.de/pub.
(27) Becke, A. D. *J. Chem. Chem.* **1993**, *98*, 5648.
(28) Lee, C.; Yang, W.; Parr, R. G. *Phys. Rev. B* **1988**, *37*, 785.
(29) Sinnecker, S.; Slep, L. D.; Bill, E.; Neese, F. *Inorg. Chem.* **2005**, *44*, 2245.
(30) Gütlich, P.; Link, R.; Trautwein, A. X. In *Inorganic Chemistry Concepts*; Becke, M., Jørgensen, C. K., Lappert, M. F., Lippard, S. J., Magrave, J. L., Niedenzu, K., Parry, R. W., Yamatera, H., Eds.; Springer-Verlag: Heidelberg, 1978; Vol. 3.

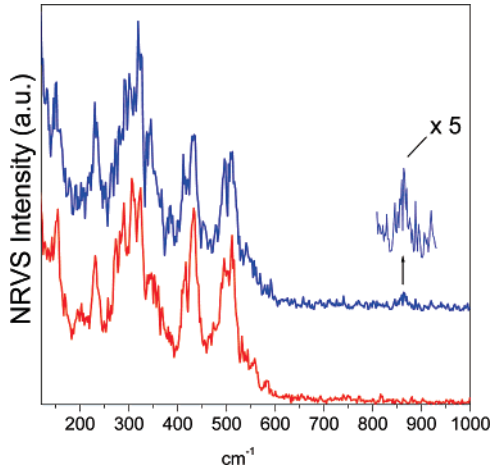

Figure 1. Experimental NRVS spectra of the lower valent Fe(III)−azide precursor (red) and the photolysis product (blue) ($T = 20$ K).

Although intuitively it is expected that this vibrational mode must arise from the ν_{Fe-N} stretching mode, we have performed a much more careful analysis of the NRVS spectra on the basis of detailed DFT calculations.

Calculations and Assignments. The NRVS intensity derives exclusively from ^{57}Fe nuclei and directly depends on the vibrational frequencies and normal mode composition factors that characterize the extent of involvement of the resonant nucleus in a given normal mode.[10,31] The normal mode composition factors of ^{57}Fe (denoted as $e^2_{Fe\alpha}$, where index α refers to a normal mode) are determined by the molecular force fields, and thus their values reflect the details of the electronic structure. In particular, the differences in bonding result in the noticeable variations of the NRVS intensity pattern between the species **1** and **2**, as one can see from Figure 1.

In order to arrive at a detailed assignment of the spectra, we have carried out a multistep analysis that combines elements of least-squares fitting and electronic structure calculations. The fit was done in the spectral range 130−1000 cm^{-1}. The spectral region below 130 cm^{-1} has almost unresolved structure due to the presence of rather intense low frequency and acoustic bands, and therefore was excluded from further consideration. The subtraction of a broad featureless background was necessary as well. Such a background may arises from two major factors: (a) secondary electron scattering processes, whereby the nuclear scattering observed in the NRVS experiment is not completely separated from the electronic one and (b) acoustic phonons that are co-excited with the molecular vibrations under consideration.[10]

In order to put the fitting on as sound as possible physical ground, we have carried out DFT frequency calculations performed at the BP86/TZVP level of theory. The DFT calculations provide the number of vibrational modes in the investigated frequency range, as well as initial guesses for the normal mode composition factors $e^2_{Fe\alpha}$ (according to eqs 1−11 in the Supporting Information) and vibrational frequencies. In order to avoid ambiguities and to minimize the number of free parameters, all linewidths (FWHM, full width at half-height) were kept identical. After initial trials, the line shape was determined to be better represented by Lorentzians than by Gaussians, with a FWHM of 15.1 cm^{-1}.

(31) Sage, J. T.; Paxson, C.; Wyllie, G. R. A.; Sturhahn, W.; Durbin, S. M.; Champion, P. M.; Alp, E. E.; Scheidt, W. R. *J. Phys.: Condens. Matter* **2001**, *13*, 7707.

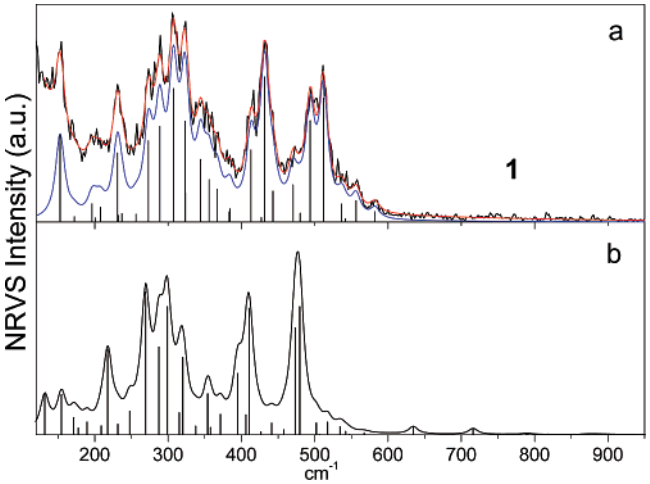

Figure 2. Experimental (a, black curve), fitted (a, red), and simulated (b) NRVS spectrum of the Fe(III)−azide precursor obtained at the BP86/TZVP level ($T = 20$ K). Bar graphs represent the corresponding intensities of the individual vibrational transitions. The blue curve represents the fitted spectrum with a background line removed.

According to the DFT calculations, there are 33 and 31 vibrations in the range 130−600 cm^{-1} for **1** and ^{2,4}**2**, respectively. Nearly all experimental and calculated NRVS intensity is in this region. Indeed, as follows from the normal-mode analysis (*vide infra*), all vibrations with significant involvement of Fe motion actually fall into this range. For species ^{2,4}**2**, there also is a band at higher frequency. Consistent with this finding, the sum of the Fe normal mode composition factors corresponding to the spectral region 130−600 cm^{-1} is >2.1 for all species **1**, ^{2}**2**, and ^{4}**2**, which is not much less than the value of ∼2.5 corresponding to the sum of all non-trivial normal modes. Thus, 33 normal modes in the range 130−600 cm^{-1} were included in the fit for species **1,** and 32 for species **2.** Because only relative NRVS intensities were fit, the variations of $e^2_{Fe\alpha}$ were performed such that the sum over all modes included in the fit was kept equal to the corresponding value obtained from the DFT calculations. Problems with fitting occur for lines within $\Delta\nu \approx 10$ cm^{-1}, which are not well-resolved in the experiment. In this case, the intensity ratio of the peaks was kept at the quantum chemically calculated ratio.

Figure 2 presents experimental, fitted, and purely quantum-chemically calculated NRVS spectra of the ferric-azide complex **1**. It is obvious that the fitted trace describes the experimental spectra within the signal-to-noise ratio perfectly. Furthermore, the purely theoretical spectrum is in very nice agreement with the fitted spectrum. This indicates that the calculations provide a highly realistic force field and normal mode composition factors for **1** and are invaluable as a guide for least-square fittings.

The fitted and calculated vibrational frequencies and normal mode composition factors corresponding to the 18 most important NRVS bands as well as their approximate correlation between the species **1** and **2** are presented in Table 1. It is evident that the vibrational peaks in the calculated NRVS spectrum are typically 0−30 cm^{-1} too low compared to the experimental values. In the calculated NRVS spectra, there are two small peaks at 635 and 716 cm^{-1} (Figure 2b) that are not visible in the experimental spectrum. According to the normal mode calculations these are Fe−N−N and Fe−O−C deformation vibrations. Small admixtures of Fe−N and Fe−O stretching modes account for the calculated nonzero normal mode com-

Table 1. Experimental and Calculated at the BP86/TZVP Level Frequencies and Corresponding Values of the Iron Normal Mode Composition Factors of the Most Important Vibrations That Appear in the NRVS Signal of the Fe(III)−Azide Precursor **1**, and the Photolysis Product **2**, and Their Approximate Correlation between the Different Species

	Fe(III)–azide (**1**)				Fe–(V)–nitrido (**2**)					
	frequency		$e^2_{Fe\alpha}$		frequency			$e^2_{Fe\alpha}$		
vibration	calc.	exp.	calc.	exp.	calc. $S = {}^3/_2$ (^{4}**2**)	calc. $S = {}^1/_2$ (^{2}**2**)	exp.	calc. $S = {}^3/_2$ (^{4}**2**)	calc. $S = {}^1/_2$ (^{2}**2**)	exp.
ν_1 N−Fe−N bending	131.7	153	0.029	0.06	129.7	130.3	162	0.041	0.067	0.05
ν_2 N−Fe−N bending	171.1	196	0.016	0.02	190.5	189.2	218	0.091	0.036	0.04
ν_3 N−Fe−N bending	189.4	207	0.014	0.02	191.4	165.8	179	0.101	0.01	0.02
ν_4 N−Fe−N bending	217.7	231	0.098	0.07	216.2	200.6	232	0.122	0.118	0.11
ν_5 N−Fe−N bending	231.5	256	0.013	0.01	221.7	224.9	242	0.068	0.062	0.06
ν_6 N−Fe−N bending	269.2	273	0.205	0.10	252.0	268.9	295	0.268	0.277	0.18
ν_7 N−Fe−N bending N−Fe stretching	287.4	289	0.135	0.12	300.2	303.9	320	0.087	0.219	0.23
ν_8 N−Fe−N bending N−Fe stretching	298.9	307	0.205	0.19	278.5	321.9	343	0.188	0.15	0.15
ν_9 N−Fe−N bending Fe−N stretching	315.2	323	0.037	0.04	313.0	312.4	328	0.098	0.131	0.14
ν_{10} N−Fe−N bending	319.9	323	0.132	0.15	269.7	287.5	295	0.274	0.137	0.05
ν_{11} Fe−N stretching	354.0	356	0.078	0.07	332.0	324.2	343	0.116	0.044	0.05
ν_{12} N−Fe−N bending	357.7	367	0.014	0.05	349.6	368.8	387	0.017	0.067	0.03
ν_{13} Fe−N stretching	394.8	413	0.129	0.13	410.0	425.21	455	0.019	0.046	0.10
ν_{14} Fe−N stretching	410.5	432	0.278	0.28	452.06	443.6	497	0.114	0.076	0.12
ν_{15} Fe−N stretching	426.6	443	0.007	0.06	358.1	393.8	418	0.123	0.071	0.13
ν_{16} Fe−N stretching	473.4	494	0.272	0.23	444.4	471.2	517	0.129	0.304	0.26
ν_{17} Fe−N stretching Fe−O stretching	479.5	512	0.328	0.29	385.3	365.2	387	0.101	0.108	0.05
ν_{18} Fe−N stretching	634.5	—	0.028	—	670.7	937.3	864	0.138	0.144	0.16

position factors. Although the calculated relative intensities are slightly above the detection limit dictated by the signal-to-noise ratio, they are determined by values of $e^2_{Fe\alpha}$ that are very small (0.028 and 0.026 for the peaks at 635 and 716 cm^{-1}, respectively) and they must be considered to be within the uncertainties of the theoretical treatment. According to the comparison between fitted and calculated normal mode composition factors, the calculations have an accuracy of about 0.02 for $e^2_{Fe\alpha}$ compared to the most intense features, which have $e^2_{Fe\alpha} \approx 0.3$.

After the detailed analysis was performed for the NRVS data of Fe(III)−azide precursor **1**, it became possible to quantitatively interpret the NRVS spectra of the photolysis product **2** (Figure 1). In principle, the observation of a band at 864 cm^{-1} in the experimental spectrum of the photolysis product, together with the previously presented data analysis,[7] provides the primary evidence in favor of $S = {}^1/_2$ (^{2}**2**) state rather than the $S = {}^3/_2$ (^{4}**2**) assignment. The calculated normal mode composition factors of the high-frequency Fe−N stretching mode ν_{18} are almost the same for both spin states. Thus, the NRVS spectrum should be observable for either case. However the predicted frequency for ^{4}**2** (ν_{18} = 671 cm^{-1}) shows a much larger discrepancy with the observed fundamental frequency of 864 cm^{-1} than in the case of ^{2}**2** (ν_{18} = 937 cm^{-1}). The latter value corresponds to an error of ∼8%, which is well within the error range of 0−13% observed for the calculated frequencies of the Fe(III)−azide precursor **1** (Table 1). The relative error of 22% corresponding to ^{4}**2** is outside this range. This is consistent with a detailed statistical analysis of the typical errors in vibrational frequencies calculated using the BP86 functional.[32]

In order to obtain an even more detailed analysis of the experimental data, we have performed a fit of the experimental NRVS spectrum of the photolysis product which contains a mixture of **1** and **2**. Because the exact conversion ratio of **1** to **2** was not known *a priori*, the species abundances were also varied in the fitting procedure while the vibrational frequencies and normal mode composition factors of **1** were kept fixed to the values obtained in the previous fit. As further evidence in favor of ^{2}**2** ground state, it should be noted that the calculated parameters for ^{4}**2** did not provide a good initial guess for the fitting procedure. In particular, the intense bands around 320 cm^{-1} (which account for the major changes between **1** and **2** in the spectral range below 500 cm^{-1}) do not appear in the calculated NRVS spectrum of ^{4}**2**.

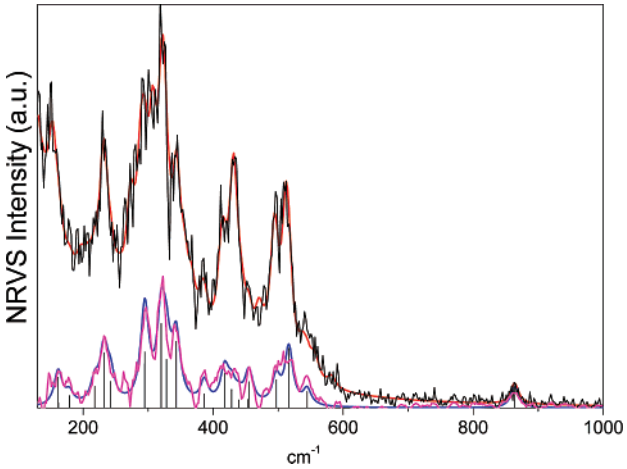

Figure 3. Experimental (black curve), fitted (red) NRVS spectrum of the photolysis product. The magenta curve represents the smoothed component of the experimental spectrum corresponding to the species **2**. The blue curve is the simulated spectrum of **2** corresponding to the fitted parameters. Bar graphs represent the intensities of the individual vibrational transitions.

The fitted vibrational frequencies and normal mode compostion factors of **2** are given in Table 1. The fitted value of the fractional contribution of **2** to the NRVS spectrum is 32% Fe(V) (and 68% of **1**), which corroborates the initial estimate. Figure 3 represents the "experimental" spectrum of a pure species **2**, which was obtained by subtraction of the simulated spectrum of **1** (corresponding to its fitted abundance from the

(32) Scott, A. P.; Radom, L. *J. Phys. Chem. B.* **1996**, *100*, 16502.

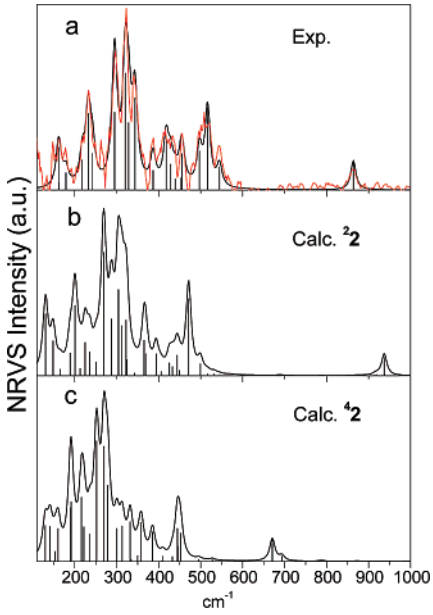

Figure 4. Experimental smoothed (a, red curve), fitted (a, black) NRVS spectrum of the species **2**. The calculated (BP86/TZVP level) NRVS spectra of the species ^{2}**2** and ^{4}**2** are given in (b) and (c), respectively. Bar graphs represent the intensities of the individual vibrational transitions.

measured experimental spectrum of the mixed photolysis product) and a background line. This spectrum should accurately correspond to the nitrido-species **2**. It was additionally smoothed by a 5-point Savitzky−Golay procedure.[33]

Figure 4 shows comparison between the experimental, fitted, and theoretical NRVS spectra obtained for species ^{2}**2** and ^{4}**2**. The calculated NRVS spectrum of ^{2}**2** is in reasonable agreement with the experimental one, whereas the spectrum calculated for ^{4}**2** shows a much larger discrepancy along the entire spectral envelope. In particular, the most intense bands for $S = {}^3/_2$ are typically down-shifted relative to their counterparts for the low-spin species which is related to the strengthening the Fe−N_{eq} bonds in the latter case (*vide infra*).

Take together, the detailed analysis of the NRVS data allows us to conclusively identify the photoproduct as the desired target species **2** and to unambiguously identify its spin state as being $S = {}^1/_2$ (^{2}**2**) rather than $S = {}^3/_2$ (^{4}**2**). This, of course, is consistent with the previous analysis.[7]

Normal Mode Compositions. The normal-mode analysis has shown that in the case of **1** and ^{2,4}**2** species there are ∼18 vibrational modes that are characterized by significant involvement of the Fe nucleus (i.e., large values of $e^2_{Fe\alpha}$). The frequencies and normal mode composition factors corresponding to these vibrations, as well as their correlation between different species, are described in Table 1.

The shapes of the most important normal modes in the vicinity of the core region around the Fe atom are shown in Figure 5. The entire set of vibrations that are active in the NRVS may be roughly partitioned into three groups: (1) N−Fe−N bending vibrations (spanning the spectral region 100−300 cm^{-1}); (2) mixed modes involving N−Fe−N bending and Fe−N stretching (300−400 cm^{-1}); (3) Fe−N stretching vibrations (>400 cm^{-1}). The in-plane Fe−N stretching modes ν_{13}−ν_{17} appear in the range ∼400−600 cm^{-1}, whereas the out-of-plane ν_{18} mode

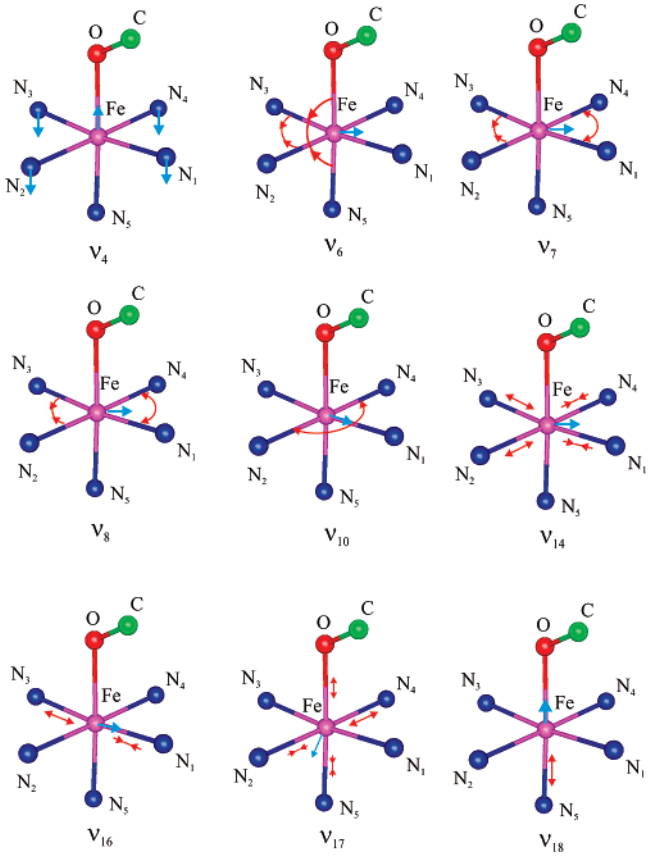

Figure 5. Schematic representation of the normal modes of Fe(III)−azide (**1**) and Fe(V)−nitrido (**2**) species with the largest iron composition factors. The individual displacements of the Fe nucleus are depicted by a blue arrow. All vibrations except for ν_4 are characterized by a significant involvement of bond stretching and bending coordinates (red arrows and arch-lines). In such a case, the length of the arrows and arch-lines roughly indicate the relative amplitude of bond stretching and bending, respectively. Internal coordinates vibrating in antiphase are denoted by inward and outward arrows respectively.

involving the Fe−N_5 bond stretching has a higher frequency in all compounds.

Fe−N_{axial} Stretching Vibration. The ν_{18} ($\equiv\nu_{FeN}$) vibration has proven to be a key spectral marker for the spin state of the photolysis product **2**. The Fe−N_5 bond stretch contributions to different normal modes may be characterized by the value of the normal mode partitioning function P^i_{FeN} defined as:

$$P^i_{FeN} = (\mathbf{D}_{FeN}\mathbf{Q}^i)^2/(\mathbf{D}_{FeN}{}^2\,(\mathbf{Q}^i)^2 \qquad i \in [1,3N-6] \quad (1)$$

where all the vectors are defined in Cartesian mass-weighted coordinates, $\mathbf{D}_{FeN}$ is a 3*N*-component unit vector that represents a purely diatomic stretching normal mode between atoms Fe and N_5 and $\mathbf{Q}^i$ is the *i*-th molecular normal mode. One can easily see that $\sum_{i=1}^{3N-6} P^i_{FeN} = 1$. The ν_{18} vibration is characterized by significant values of the Fe−N_5 partitioning function for **1** and **2** (Table 2). Accordingly, the frequency of the ν_{18} mode is to a large extent determined by the Fe−N_5 force constant. We have calculated the approximate quasi-diatomic force constant k_{FeN} from the Cartesian force constant matrix **F** by the equation $k_{AB} = -\sum_{\mu,\nu} t_\mu t_\nu F_{A_\mu B_\nu}$ where $t = (\mathbf{R}_A - \mathbf{R}_B)|\mathbf{R}_A - \mathbf{R}_B|^{-1}$ and $\mathbf{R}_A$ and $\mathbf{R}_B$ denote the positions of atoms *A* and *B*. According to the DFT ground-state force field calculations, the force constant of the Fe−N_5 bond of the Fe(V)−nitrido complex in the $S =$

(33) Savitzky, A.; Golay, M. J. E. *Anal. Chem.* **1964**, *36*, 1627.

Table 2. Bond Distances (R_{FeN}) and Quasi-Diatomic Force Constants for the Fe−N_5 Bond, Frequencies of the ν_{18} Mode, and Corresponding Values of the Diatomic Normal Mode Partitioning Function for the Fe(III)−Azide Precursor and the Photolysis Products[a]

	Fe(III)–azide (**1**)	Fe–(V)–nitrido $S = {}^1/_2$ (^{2}**2**)	Fe–(V)–nitrido $S = {}^3/_2$ (^{4}**2**)
R_{FeN}	1.934	1.609	1.738
k_{FeN}(mDyne/Å)	1.10	5.40	2.40
ν_{18}	634.5	937.3	670.7
$P_{FeN}{}^{18}$	0.17	0.75	0.85

[a] Values were obtained at the BP86/TZVP level of theory.

$^1/_2$ spin state (^{2}**2**) is approximately two times larger than for $S = {}^3/_2$ spin state (^{4}**2**) (Table 2). The reason for this change is obvious from the electronic configurations in the two spin states. In the $S = {}^3/_2$ state, each orbital in the t_{2g} subshell d_{xz},d_{yz}, and d_{xy} is occupied by one spin-up electron. However, the d_{xz} and d_{yz} iron orbitals are involved in an extremely strong antibonding π-interaction with the strongly electron donating nitrido ligand.[7] On the other hand, the d_{xy} based orbital is completely nonbonding. In the $S = {}^1/_2$ state, the d_{xy} orbital becomes doubly occupied with only one electron occupying the nearly degenerate ($d_{xz,yz}$) set. Thus, the loss of a strongly antibonding interaction accounts for an increase of the force constant by a factor of 2 by going from $S = {}^3/_2$ to $S = {}^1/_2$.

As discussed previously,[7] the enormous antibonding π-interaction is also responsible for the very large $d_{xy}/d_{xz,yz}$ splitting of more than 2 eV observed in the calculations, which is ultimately also responsible for the energetic preference of the system for the $S = {}^1/_2$ state. The large differences in the force constants of ^{2}**2** and ^{4}**2** are directly reflected in the predicted vibrational frequencies of the ν_{18} mode. In ^{2}**2** it is calculated as 937 cm^{-1} (the experimental value is 864 cm^{-1}), which is noticeably higher than the calculated value of 671 cm^{-1} found for ^{4}**2**. The rather large calculated value of the normal mode composition factor, of approximately 0.14 for both species, renders the mode ν_{18} detectable in the NRVS measurements. Thus, the observation of the pronounced peak at 864 cm^{-1} in the NRVS signal of the photolyzed sample leads to the conclusion that the photolysis product is a genuine Fe(V) compound with ground state doublet multiplicity, in nice agreement with the Mössbauer, XAS and SQUID results presented previously.[7]

Anharmonic Corrections to the Fe−N Stretching Frequency. In an effort to elucidate the origin of the significant discrepancy between the calculated harmonic (937 cm^{-1}) and the experimental (864 cm^{-1}) frequencies for the ν_{18} mode, we have calculated the leading anharmonic correction Δ_{18} for this vibration. Δ is defined such that $\nu = \omega + \Delta$, where ω and ν are harmonic and fundamental frequencies, respectively. Because this mode involves primarily Fe−N_5 bond stretch, it was assumed that the anharmonicity is dominated by diagonal contributions to vibrational Hamiltonian. Thus, anharmonic force constants were evaluated in an eight-step scan of the ground-state potential energy surface along the ν_{18} mode at the BP86/TZVP level of theory, which was shown to reproduce experimental anharmonic contributions very accurately.[34,35] Anharmonic force constants were calculated through a fit of the ground-state potential energy of the form given in eq 2 to the energies evaluated at displaced geometries:

$$U = U_0 + \frac{\omega}{2}q^2 + \frac{b_3}{6}q^3 + \frac{b_4}{24}q^4 \qquad (2)$$

where b_3 and b_4 are cubic and quartic force constants, respectively, and q is the dimensionless normal coordinate for the ν_{18} mode. The calculated potential energy function along the ν_{18} mode shows a pronounced anharmonicity. Thus, over the sampled region, the average deviation between the calculated and fitted potential curve decreases from 0.0036 E_h ($b_3 = b_4 = 0$) to 0.00006 E_h ($b_3 \neq 0, b_4 \neq 0$). The final values $b_3 = 203.7$ cm^{-1} and $b_4 = 29.5$ cm^{-1} were obtained from the fit. The diagonal contribution to the anharmonic correction was calculated with two methods. Using the results of perturbation theory it may be obtained as follows:[36]

$$\Delta = \frac{1}{8}\left(b_4 - {b_3}^2\frac{5}{3\omega}\right) \qquad (3)$$

Alternatively, Δ may be calculated more rigorously through the diagonalization of the vibrational Hamiltonian ($\hat{H} = (\omega/2)[-(\partial^2/\partial q^2) + q^2] + (b_3/6)\,q^3 + (b_4/24)\,q^4$) in a basis of Hermitian functions. In this case, the anharmonic correction was evaluated from the energy difference between the first excited and the ground-state vibrational levels. The results are already fully converged with a basis of only five vibrational basis functions. Both methods provided virtually identical values of Δ around -5.5 cm^{-1}. Thus, the difference of ~ -74 cm^{-1} between the experimental and calculated frequencies for the ν_{18} mode is due to the error intrinsic to the chosen DFT/basis set combination (BP86/TZVP) rather than to the effects of anharmonicity. We do not expect this conclusion to change upon inclusion of off-diagonal contributions to the anharmonic correction.

The calculations also show that the NRVS signal (for all considered species at the given temperature ($\sim$20 K)) is dominated by contributions from fundamental transitions, whereas the total relative intensities of the various overtone and combination bands constitute less than 2.5% of the signal (not shown).

PVDOS. The partial vibrational density of states (PVDOS) for the species **1** and ^{2}**2** (constructed according to eq 10 in Supporting Information on the basis of the fitted vibrational frequencies and normal mode composition factors) is shown in Figure 6. The PVDOS directly characterizes the involvement of the Fe nucleus in different normal modes and provides a graphical representation of the calculated normal mode composition factors. One can see that for the species ^{2}**2** the PVDOS is to a large extent eliminated in the 400−550 cm^{-1} range compared to the Fe(III)−azide precursor **1**, which occurs due to the larger contribution of the Fe nucleus in the lower-frequency modes.

Conclusions and Discussion

In summary, the NRVS spectra, together with a first principles analysis of the data, unambiguously confirm that the 864 cm^{-1} feature is due to the Fe−N_{axial} stretching vibration in complex **2**. These results are in agreement with previously reported XAS, Mössbauer, magnetic susceptibility, and DFT calculations, and

(34) Neugebauer, J.; Hess, B. *J. Chem. Phys.* **2003**, *118*, 7215.
(35) The step size in dimensionless normal coordinates Δq has been chosen such that the expected total energy change due to the purely harmonic contribution was 0.002 Eh. Thus, the displacement Δq18 was 0.97, and the potential energy was scanned in the range from −3.87 to 3.87 of dimensionless normal coordinates. This range roughly corresponds to the expected region of localization of the wavefunctions describing the first two vibrational levels. The latter are needed to evaluate Δ.
(36) Mills, I. M. In *Molecular spectroscopy: modern research*; Rao, K. N., Mathews, C. W., Eds.; Academic Press: New York, 1972; Vol. 1, pp 115−140.

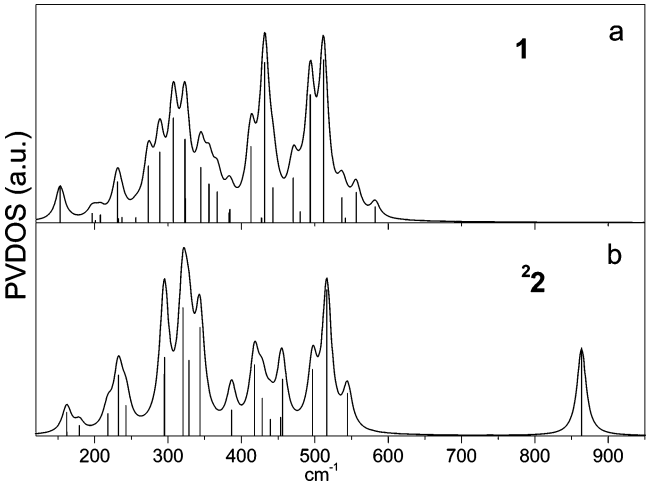

Figure 6. PVDOS of the species **1** and ^{2}**2** corresponding to the vibrational frequencies and normal mode composition factors obtained from the fit.

provide further evidence for an $S = {}^1/_2$ ground state in the Fe(V)−nitrido complex.[7] Importantly, these results provide the first experimental measure of the Fe−N stretch in **2**.

It is of interest to compare the vibrational data obtained for **2**, to that of other high-valent Fe complexes. Of particular relevance is a comparison of our results to the Fe(V)−nitrido porphyrin complexes, synthesized by Wagner and Nakamoto.[37,38] Similar to **2**, these complexes are generated by photolysis of a lower valent Fe(III)−azide precursor (either Fe(OEP)(azide) or Fe(TPP)(azide), where OEP = octaethylporphyrin and TPP = tetraphenylporphyrin). The resultant Fe(V)−nitrido−porphyrin species is extremely unstable; however, characterization by resonance Raman showed an 876 cm^{-1} band, which was assigned as an Fe(V)−N stretch. This is in very close agreement with the 864 cm^{-1} Fe−N stretch obtained for **2**, and would seem to support and low spin Fe(V) ground state for the Fe(V)−porphyrin species (rather than the previously proposed $S = {}^3/_2$ ground state).[38,39] However, in the absence of additional spectroscopic and/or structural characterization, this assignment is difficult to make, as the absence (or presence) of a trans axial ligand in the Fe(V)−porphyrin, as well as the possibility of a porphyrin π-cation radical, could also make a contribution to the Fe−N(axial) frequency.[39] It would therefore appear to be worthwhile to reinvestigate this unique species experimentally.

Manganese(V)−nitrido analogues of both complex **2** (i.e., Mn(V)(N)(cyclam−Ac)) and the Fe(V)(N)(TPP) complexes are known.[40,41] The stretching frequencies for Mn(V)(N)(cyclam−Ac) and Mn(V)N(TPP) are 1011 cm^{-1} and 1052 cm^{-1}, respectively.[37,40] In both cases, the increased M−N stretching frequency for the Mn complexes relative to their Fe analogues may be attributed to the fact the in low spin d^2 Mn(V) only the nonbonding d_{xy} orbital is occupied. On going to the Fe complexes, the π-antibonding (d_{xz} and/or d_{yz}) orbitals become occupied, decreasing the strength of this interaction. The extent of the effect will depend on the spin state of the Fe (i.e., $S = {}^1/_2$ or $S = {}^3/_2$, vide infra). The contribution of the ground state electron configuration to the observed Fe−N(nitrido) stretch is also clearly observed by comparison of **2** to the Fe(IV)(N)[PhBP$^{iPr}_3$] complex synthesized by Betley and Peters.[42] This complex has an unusual Fe(IV), $S = 0$ ground state, where the d_{xy} and $d_{x^2-y^2}$ orbitals are both doubly occupied and nonbonding. This results in formally an Fe−N triple bond, with an even higher Fe−N stretching frequency (1034 cm^{-1}) than that observed for **2**.[43,44]

Recently, Berry et al. have synthesized and characterized the first octahedral coordination compound of Fe(VI).[6] The Fe(VI) complex is analogous to **2**, having a nitrido ligand and employing a methylated cyclam-acetato ligand. This species has been characterized by Mössbauer and XAS, with the aid of DFT calculations, as an $S = 0$ Fe(VI) species with a 1.57 Å Fe−N triple bond. Though the Fe−N stretching frequency has not been observed experimentally, it is calculated at a frequency of 1064 cm^{-1}. This is fully consistent with an electronic configuration in which only the nonbonding d_{xy} orbital is doubly occupied, thus strengthening the Fe−N(nitrido) bond relative to **2**. As this is another case where conventional vibrational methods have failed to give a measure of the Fe−N stretching frequency, NRVS should again provide an ideal means for obtaining this information.

In conclusion, we have obtained NRVS data for **1** and **2** and have successfully fitted and simulated the data using a DFT approach. The combined experimental and theoretical results allow for the unambiguous assignment of **2** as an $S = {}^1/_2$ ground state. Comparison of these results to vibrational data on related high-valent iron compounds provides further support for the ground state electronic structure description, and is fully consistent with Mössbauer, magnetic susceptibility, and XAS spectroscopic studies.[7] Further, the sensitivity of NRVS to iron dynamics provides promise for future characterization of additional high-valent iron species in both model and protein systems.

Acknowledgment. The Advanced Photon Source is supported by the DOE, Basic Energy Sciences, Office of Science, under Contract No. DE-AC02-06CH11357. S.D.G. acknowledges SSRL for funding. SSRL operations are funded by the Department of Energy, Office of Basic Energy Sciences. The Structural Molecular Biology program is supported by the National Institutes of Health, National Center for Research Resources, Biomedical Technology Program and by the Department of Energy, Office of Biological and Environmental Research. T.P. and F.N. acknowledge the financial support from the Rheinische Friedrich-Wilhelms-Universität, Bonn, Germany, the Max-Planck Gesellschaft, and the priority program 1137 of the German Science Foundation.

Supporting Information Available: Figure S1 and protocol for spectral simulation of NRVS and PVDOS. This material is available free of charge via the Internet at http://pubs.acs.org.

JA070792Y

(37) Wagner, W.-D.; Nakamoto, K. *J. Am. Chem. Soc.* **1988**, *110*, 4044.
(38) Wagner, W.-D.; Nakamoto, K. *J. Am. Chem. Soc.* **1989**, *111*, 1590.
(39) Nakamoto, K. *Coord. Chem. Rev.* **2002**, 153.
(40) Grapperhaus, C. A.; Bill, E.; Weyhermüller, T.; Neese, F.; Wieghardt, K. *Inorg. Chem.* **2001**, *40*, 4191.
(41) Hill, C. L.; Hollander, F. J. *J. Am. Chem. Soc.* **1982**, *104*, 7318.
(42) Betley, T. A.; Peters, J. C. *J. Am. Chem. Soc.* **2004**, *126*, 6252.
(43) Mehn, M. P.; Peters, J. C. *J. Inorg. Biochem.* **2006**, *100*, 634.
(44) Mehn, M. P.; Brown, S. D.; Jenkins, D. M.; Peters, J. C.; Que, L., Jr. *Inorg. Chem.* **2006**, *45*, 7417.
(45) Higher frequency data have been reported for the Fe−D stretch in [FeH(D)$_6$][MgBr(THF)$_2$]$_4$: Bergmann, U.; Sturhahn, W.; Linn, D. E., Jr.; Jenney, F. E., Jr.; Adams, M. W. W.; Rupnik, K.; Hales, B. J.; Alp, E. E.; Mayse, A.; Cramer, S. P. *J. Am. Chem. Soc.* **2003**, *125*, 4016.